Effect of nitrogen/phosphorus concentration on algal organic matter generation of the diatom *Nitzschia palea*: Total indicators and spectroscopic characterization

Linlin Han[1], Bingbing Xu[2,*], Fei Qi[1,*], Zhonglin Chen[3]

1. Beijing Key Laboratory for Source Control Technology of Water Pollution, College of Environmental Science and Engineering, Beijing Forestry University, Beijing 100083, China. E-mail: linlinhan163@163.com
2. State Key Laboratory of the Environmental Criteria and Risk Assessment, Chinese Research Academy of Environmental Sciences, Beijing 100012, China
3. State Key Laboratory of Urban Water Resource and Environment, Harbin Institute of Technology, Harbin 150090, China

ARTICLE INFO

ABSTRACT

Critical algal blooms in great lakes increase the level of algal organic matters (AOMs), significantly altering the composition of natural organic matters (NOMs) in freshwater of lake. This study examined the AOM's characteristics of *Nitzschia palea* (*N. palea*), one kind of the predominant diatom and an important biomarker of water quality in the great lakes of China, to investigate the effect of AOMs on the variation of NOMs in lakes and the process of algal energy. Excitation–emission matrix fluorescence (EEM) spectroscopy, synchronous fluorescence (SF) spectroscopy and deconvolution UV–vis (D-UV) spectroscopy were utilized to characterize AOMs to study the effects of nutrient loading on the composition change of AOMs. From results, it was revealed that the phosphorus is the limiting factor for *N. palea*'s growth and the generation of both total organic carbon and amino acids but the nitrogen is more important for the generation of carbohydrates and proteins. EEM spectra revealed differences in the composition of extracellular organic matter and intracellular organic matter. Regardless of the nitrogen and phosphorus concentrations, aromatic proteins and soluble microbial products were the main components, but the nitrogen concentration had a significant impact on their composition. The SF spectra were used to study the AOMs for the first time and identified that the protein-like substances were the major component of AOMs, creating as a result of aromatic group condensation. The D-UV spectra showed carboxylic acid and esters were the main functional groups in the EOMs, with $-OCH_3$, $-SO_2NH_2$, $-CN$, $-NH_2$, $-O-$ and $-COCH_3$ functional groups substituting into benzene rings.

© 2016 The Research Center for Eco-Environmental Sciences, Chinese Academy of Sciences. Published by Elsevier B.V.

Introduction

In recent years, global climate change led to several hydrological geology disasters in great lakes such as the shrinkage and significant temperature increases that concentrated pollutants and aggravated lake eutrophication, resulted in frequent algal blooms in fresh water lakes and reservoirs (Glibert et al., 2014). Many algal bloom events have been reported in China's great lakes or reservoirs in recent years (Liu et al., 2011b), each of which is followed by a huge release

---

* *Corresponding authors.* E-mails: xbb_hit@126.com (Bingbing Xu), qifei@bjfu.edu.cn, qifei_hit@163.com (Fei Qi).

of algal organic matter (AOM). As a major contributor to the natural organic matter (NOM) in lakes, these huge inputs of AOMs can have a big impact on a lake's NOM composition because of their different properties (Henderson et al. 2008a). In addition to destroying the geochemical composition of water bodies (Henderson et al., 2010), it also affects their aqueous water chemical behavior (Beaulieu et al., 2005; Vandamme et al., 2012). Generally, AOMs in surface water or lake, would be accounted for color, taste and odor (Dokulil and Teubner, 2000) and can lead to the production of hazardous cyanobacteria toxins. When lakes and reservoirs are used as source water, these variations of the NOM composition will also influence drinking water treatments including coagulation (Alizadeh Tabatabai et al., 2014; Henderson et al., 2010), filtration (Taylor Eighmy et al., 1992) and disinfection (Fang et al., 2010). The released AOM is not totally consumed by the heterotrophic bacteria in lakes, resulting in its concentration buildup. Recently, algal were used as an economic source for biofuel. The composition of algal will influence the harvesting-extraction systems and energy conversion efficiency. It is therefore necessary to assess how AOM in lakes is generated and how its composition changes during or after an algal bloom to better understand the resulting change in a lake's NOM, effects on subsequent drinking water treatment and algae biomass process.

The released AOM is composed of the extracellular organic matter (EOM) releasing from the algal cell and intracellular organic matter (IOM) from cell autolysis, generated during population growth and would be released after dead. Generally, the AOM is mainly composed of polysaccharides, proteins (González López et al., 2010), peptides, amino acids and other organic acids such as fatty acids (Cardozo et al., 2007). Several of these have been used to characterize the composition of the AOM for *Euglena gracilis*, *Microcystis aeruginosa*, *Chlorella vulgaris*, *Asterionella formosa* and *Melosira* sp. by examining their cell concentration, surface area, charge density, dissolved/total organic carbon (DOC/TOC), hydrophilic properties, carbohydrate, protein, molecular weight fractionation, specific UV absorbance (SUVA) (Labanowski and Feuillade, 2011), and UV absorbance at 254 nm (Leloup et al., 2013). However, most researchers focused on the EOM generated from the exponential or stationary phases of cyanobacteria and *chlorella* (Li et al., 2012). However, little has yet been done to characterize the properties of IOM and there have been no reports about the total amino acid content or the use of spectroscopic techniques such as synchronous fluorescence and UV–vis spectra to identify the composition of IOM under different growth phases.

Diatom, an important algal bloom species all over the world, is a useful ecological indicator of aqueous ecosystem health for the rapid growth rate and the role in aqueous food web (Chen et al., 2016), however, their AOM has rarely been characterized in either lakes or reservoirs, which will affect the aqueous quality and sediment aggregation. To date, only four marine diatom species, *Skeletonema costatum*, *Achnanthes brevipes*, *Chaetoceros affinis*, and *Cylindrotheca fusiformis*, have been characterized (Granum et al., 2002; Guerrini et al., 1998, 2000; Myklestad and Haug, 1972). The AOM composition is linked to the algae, growth phase, the age of the culture, the environmental conditions including nutrient loading (Pivokonsky et al., 2006). Although EOMs of *S. costatum* as a species of the marine

diatom (Granum et al., 2002) and AOMs of *A. brevipes* blooming in Italian lakes were studied, only the carbohydrate, chlorophyll and enzyme composition were concerned, with scant attention being paid to spectroscopic analyses.

The objective of this work was, therefore, (1) to study the characteristics of the EOM and IOM produced by *Nitzschia palea*, the predominant diatom species in lakes and reservoirs in China (Ishikawa and Furuya, 2004; Yang et al., 2012); and (2) to investigate the influence of nutrients (nitrogen or phosphorus concentration) on the AOM profile of *N. palea* for all four growth phases.

1. Materials and methods

1.1. Algae cultivation

N. palea purchased from the Chinese Research Academy of Environmental Sciences was cultured in the D1 medium (the detailed composition is shown in Appendix A Table S1) of pH = 8.00–8.15 in an incubator (25°C, 12 hr/12 hr dark/light cycle; luminance = 2200 lx), and used for subsequent experiments once the cell concentration reached 1.0×10^6 cells/mL. To study the influence of nutrient salts (type and/or concentration) on the growth of the algae and the generation of AOM, the algae cells were pretreated in a starvation culture for 3 days and then spiked into the appropriate phosphate or nitrogen medium (details of the nutrient concentration are shown in Appendix A Table S2) at an initial concentration of 1.0×10^5 cells/mL. Each treatment set consisted of three parallel samples.

1.2. AOM extraction

Centrifugal-filtration was used to extract the EOM and IOM of *N. palea*. The AOM extraction method was as follows: (a) 10 mL of cell suspension was centrifuged at 5000 r/min, 2400 ×*g* for 15 min, and the supernatant was filtered through a 0.45 μm polyethersulfone membrane filter to obtain the EOM sample (Leloup et al., 2013); (b) 10 mL ultrapure water was then added to the same volume of the residue remaining in the centrifuge tube after the EOM extraction to wash the surface of cell twice and then the residual cell was resuspended in the ultrapure water. The cells were subjected to freeze–thawing (−80°C in ultra-low freezer, 35°C in water bath) for three cycles before being centrifuged at 10,000 r/min, 9600 ×*g* for 15 min, after that the supernatant was filtered again through a 0.45 μm polyethersulfone membrane filter to obtain the IOM sample (Zhu et al., 2015). The samples were prepared up to 3 days in advance and stored in a refrigerator at 4°C until use.

1.3. AOM characterization

1.3.1. Cell concentration and specific growth rate
The cell density of the algae was determined under an optical microscope using hemocytometers every 2 days until the beginning of the decline phase. The specific growth rate (μ) is calculated as Eq. (1):

$$\mu = \frac{\ln C_t - \ln C_0}{t} \tag{1}$$

where C_0 ($\times 10^5$ cells/mL) and C_t ($\times 10^5$ cells/mL) are the concentrations of algal cells at the beginning and end, respectively, of a specific time interval t (day).

1.3.2. Total organic carbon, protein, carbohydrate and amino acid content

TOC was measured using a 3100 total nitrogen (TN)/total phosphorous (TP) analyzer (Jena, Germany). Bradford method (Servaites et al., 2012), anthrone-sulfuric (Laurentin and Edwards, 2003) and ninhydrin assays (Chutipongtanate et al., 2012) were used to determine the concentrations of the total protein, total carbohydrates and total amino acids in AOM, respectively. The bovine serum albumin (BSA), glucose and lysine were used for calibration for protein, carbohydrate and amino acids, respectively, at 595 nm, 620 nm and 570 nm, using UV/Vis spectrophotometer (T6, Purkinje general, China). The detailed procedure information of methods was shown in Appendix A Text S1.

1.3.3. Fluorescence spectroscopy

All fluorescence spectra were recorded using an F-7000 Fluorescence Spectrophotometer (Hitachi, Japan) equipped with a Xenon lamp. Excitation/emission matrix (EEM) fluorescence spectroscopy on the AOM was performed by scanning from 200 to 400 nm for the emission spectra and from 250 to 500 nm for the excitation spectra (Liu et al., 2011a) at a scan speed of 1200 m/sec; a photomultiplier tube voltage of 700 V; slit widths of 5 nm; and scanning intervals of 10 nm for both the excitation and emission monochromators. The spectral data obtained was analyzed using the fluorescence regional integration (FRI) method (Chen et al., 2003), which is shown in detail as Appendix A Text S2. Synchronous fluorescence spectra (SF) were obtained by scanning over a range from 250 to 500 nm with a constant offset ($\Delta\lambda$ = 60 nm).

1.3.4. UV–vis spectroscopy

UV–Vis spectra were recorded with an Evolution 300 spectrophotometer (Thermo Fisher Scientific, USA) over a wavelength range of 200–400 nm (He et al., 2011). The UV–Vis spectra obtained for the AOM were deconvoluted following Yan's method (Yan et al., 2013; Yan and Korshin, 2014), which is also shown in Appendix A Text S2.

2. Results and discussion

2.1. Effect of nutrient conditions on N. palea growth

The effect of nutrient conditions on the period of growth phase of N. palea is shown in Appendix A Table S3. The changed nitrogen and phosphorus concentrations impacted the growth phase of N. palea significantly. As the ambient phosphorus concentration increased from 0.01 to 0.2 to 1.0 mg/L, the growth phase of N. palea lengthened from 13 to 15 to 16 days, respectively; for nitrogen concentrations of 1, 2 and 10 mg/L, the growth phase of N. palea lasted for 13, 16 and 15 days, respectively. As the ambient phosphorus increased, the corresponding exponential phase period rose from 5, to 7 and then 9 days, respectively; for ambient nitrogen concentrations of 1, 2 and 10 mg/L, the corresponding exponential

phase period lasted for 4, 7 and 4 days, respectively. The growth rates of N. palea AOM for each of the four growth phases under different nutrient conditions are shown in Fig. 1a. The influence of nitrogen and phosphorus on N. palea's growth is mainly reflected in the adaptation and exponential phases, where the growth rates achieved their maximum values in the adaptation phase and then decreased in the exponential phase under the investigated nitrogen loading. The growth rate in the adaptation phase increased as the nitrogen concentration increased; however, the specific rate decreased below zero in both stationary and decline phases. When TN = 1 mg/L, the growth rates in both the adaptation (0.24) and exponential phases (0.22) were much closer, indicating that this nitrogen loading was not sufficient to support N. palea's growth. Being different with the effect of nitrogen, the growth rates under all phosphorus concentrations achieved their maximum values in the exponential phase, at 0.27, 0.17 and 0.16 for the phosphorus concentrations of 0.01, 0.2 and 1 mg/L, respectively. In the adaptation phase, no significant effect of phosphorus concentration increasing was observed on N. palea's growth rate. This difference between nitrogen and phosphorus suggested that nitrogen concentration was more beneficial for N. palea growth during the adaptation and exponential phases (Zhang et al., 2007). Combined with the data in Appendix A Table S3, it is clear that increasing the phosphorus concentration extended the exponential phase significantly more than was observed under the equivalent nitrogen control experiment. Generally, the phosphorus was more beneficial for N. palea growth than the nitrogen. Interestingly, phosphorus had a negative effect on growth rate in both the stationary and decline phases, which was more significant than nitrogen effect. In summary, phosphorus showed a more significant effect on N. palea's growth than nitrogen and the effect of nutrition on N. palea's growth is mainly shown in the adaptation and exponential phases.

2.2. TOC profile of N. palea's AOM

In order to investigate the EOM and IOM of N. palea quantitatively, TOC was used to express the total concentration of AOM, as shown in Fig. 1b and c. Regardless of the nutrient concentration, TOC in the EOM was consistently higher than in the IOM, indicating that N. palea released AOM throughout its growth phase, which was different from other published results on M. aeruginosa (Zhou et al., 2014). This was the first time to report the AOM as TOC of N. palea. Compared with other results on TOC of AOM calculated as ng/cell, the values obtained in this study were very lower (0.0005–0.00255 ng/cell under different nutrient loadings in stationary phase) than that generated from diatoms as Melosira sp. (0.019 ng/cell) or Asterionella fronosu (0.65 ng/cell) (Henderson et al., 2008). Even though the culture medium used was different, the values of N. palea were much higher than that in IOM or EOM of M. aeruginosa cultured in BG11 medium as 3.01×10^{-5} or 4.2×10^{-5} ng/cell, respectively (Zhou et al., 2014). Based on the above, it was concluded that though the growth rate of diatom is lower than cyanobacteria and is not the dominated species in many freshwater, the AOM generated from diatom is much higher than cyanobacteria and was
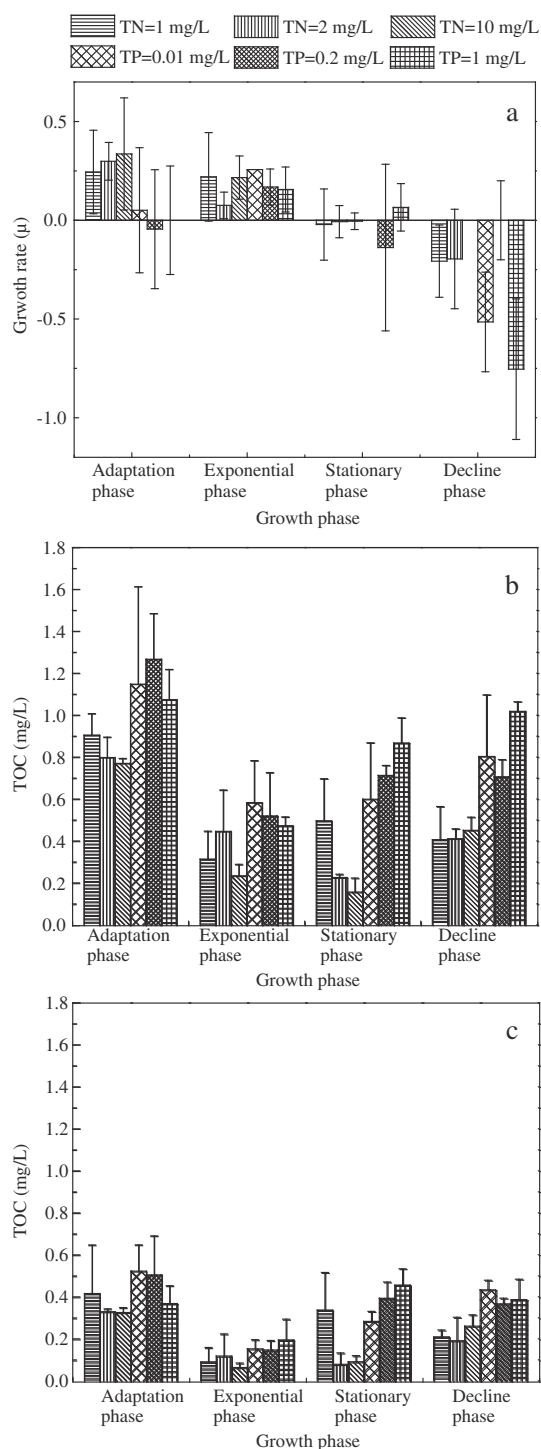
Fig. 1 – Effect of nutrient conditions on *N. palea*'s growth rate (a) in total organic carbon (TOC) variation in extracellular organic matter (EOM) (b) and intracellular organic matter (IOM) (c) under different nutrient conditions. TN: total nitrogen, TP: total phosphorous.

another important source of biological organic matters in freshwater.

Under all different nutrition loadings, TOC in both the EOM and IOM showed a significant decline from the adaptation

phase to the exponential phase. Combined with the analysis in Section 2.1, no matter what the nitrogen or phosphorus concentration was, *N. palea* reproduces mainly through consuming organic matter from AOM as it moves from the adaptation to the exponential phase. When the nitrogen concentration is as low as being 1 mg/L, TOC in the EOM appeared to go up at the transition from the exponential to the stationary phase, and then decreased in the decline phase, which contradicts the results under TN = 2 and 10 mg/L. This can be explained as follows: because of the nitrogen consuming in moving from the adaption to the exponential phase, the residual nitrogen in the environment is depleted, leaving insufficient nitrogen in the medium for *N. palea* to continue to grow during this transition (Droop, 1974; Yan and Korshin, 2014). When the environmental nutrition is scarce and some cells die, releasing TOC in the form of IOM to become part of the EOM that provides a matrix for the new growth round of the cells. This is likely the main reason for the reduction in TOC observed during the decline phase of EOM or IOM. The surviving cells store large amounts of organic matter in IOM fraction to maintain normal growth, resulting in the increasing amount of TOC in the IOM in this period. As noted in Section 2.1, when the ambient nitrogen is rich (TN = 2 mg/L), the nutrient supports the growth of *N. palea* during the adaptation and exponential phases, so the cells consume AOM and resulting in the decrease of TOC from the adaptation to stationary phases, which supports the earlier findings reported by Droop (1974) who showed that it was beneficial for *Chromulina* (a kind of cyanobacteria) growth to save protein, carbohydrates and other IOMs when nutrition was unavailable in the medium. When the ambient nitrogen was high as 10 mg/L, TOC in the IOM increased from the exponential to the stationary phase. During this period, cells of *N. palea* mainly consumed the organic matters in the EOM to maintain their growth from the exponential to the stationary phase, preserving the organic matter in their IOM and thus boosting its TOC content.

In summary, high nitrogen loading was beneficial for storing TOC in the IOM from the exponential to stationary phase; however, the effect of phosphorus concentration on the TOC profiles in AOM was more significant than that of nitrogen. Low phosphorus concentration was insufficient to allow the release of organic matter to generate EOM from the exponential to the stationary phase, while increasing the concentration was beneficial for organic matter release, resulted in the increase of TOC in EOM. Unlike EOM fraction, IOM showed an increasing trend from the exponential to the stationary phase, confirming that phosphorus is indeed beneficial by raising the TOC in IOM during this transition. The substantial cell growth supported by the sufficient supply of nitrogen led to cell death and the release of IOM to become a part of the EOM, leading to TOC in both the EOM and IOM increased from the stationary to the decline phase, regardless of the phosphorus concentration.

2.3. Carbohydrate and protein profiles in *N. palea*'s AOM

Carbohydrates and proteins are reported to be the most important components of AOM (Huang et al., 2012) and a detailed profile of the carbohydrates and proteins in *N. palea* AOM and the effect of nutrient condition is provided in Fig. S1.

To evaluate their contribution to the TOC, the ratio of carbohydrates/TOC as glucose and proteins/TOC as BSA is shown in Fig. 2. Fig. 2a shows that the amount of carbohydrate in the EOM produced by *N. palea* increased as the growth progressed and then decreased in the decline phase under all nitrogen/phosphorus concentrations. Regardless of the amount of nitrogen or phosphorus present, the highest concentration of carbohydrates was reached in the stationary phase, which supports the findings reported by other researchers (Guerrini et al., 2000). The carbohydrate yields were higher under the nitrogen control experiments than under the phosphorous ones. As the nitrogen concentration increased, the carbohydrates/TOC ratio rose sharply, but the influence of phosphorus concentrations on the carbohydrate yield was insignificant. This result indicates that nitrogen controls the generation of carbohydrates in *N. palea*. This result is not consistent with the profiles for *M. aeruginosa* (Huang et al., 2012), where the carbohydrates in the IOM were reported to be mainly produced in the exponential and stationary phases, unlike in the EOM. The increasing carbohydrate concentrations in the IOM during the exponential phase were ascribed to the cell growth (Droop, 1974; Yan and Korshin, 2014); after the nutrition was consumed, the carbohydrates in both the EOM and IOM increased in the stationary phase and carbohydrates in EOM were released from

the algae cells, leading to an increase in the IOM carbohydrates in the stationary phase (Droop, 1974; Yan and Korshin, 2014). The influence of the phosphorus on carbohydrate yield in IOM is still less than that of nitrogen. Both rich and too-rich phosphorus concentrations were beneficial for *N. palea*, preserving the carbohydrates in the EOM and IOM, although the highest yields of carbohydrates were observed for the poor phosphorus concentration. Regardless of the nutrient loading, the value of carbohydrates/TOC as glucose was much higher than 1, indicating that only very few carbohydrates generated as monosaccharide (such as glucose) and most carbohydrates generated as polysaccharide with higher molecular weight. This result was significant with previous study (Henderson et al., 2008) in that this value is closed to 1.0. Therefore, the carbohydrates generated from *N. palea* were different from *Melosira* sp. or *A. fronosu*.

As shown in Fig. 2c and d, protein generation in *N. palea*'s EOM and IOM was mainly reflected in the stationary and decline phases, with the yield of protein in the former being much higher than in the latter in both EOM and IOM. For nitrogen concentrations of 1, 2, and 10 mg/L, the proportion of protein in TOC of EOM in the stationary phase was reached to 2.23, 2.14 and 4.56, respectively. The corresponding values in IOM were 7.40, 11.23 and 6.65. The proportion of protein in
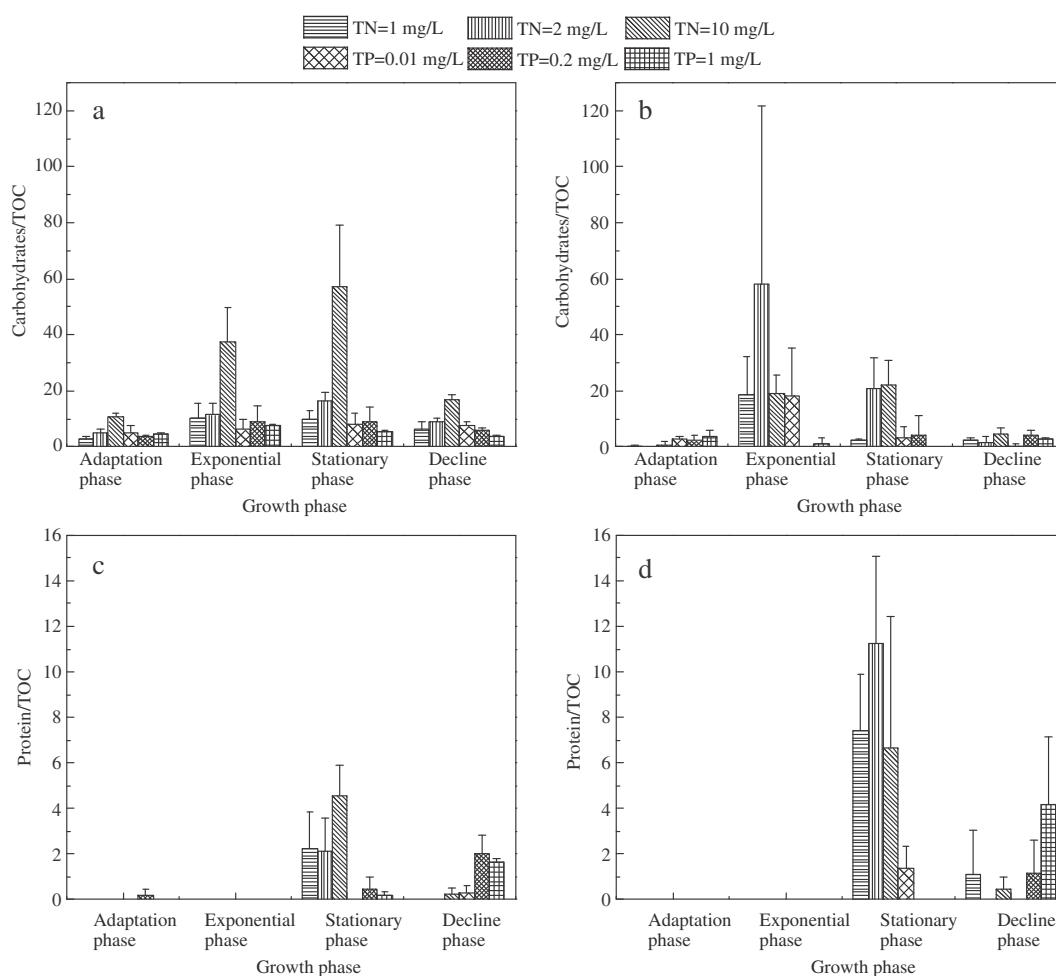

Fig. 2 – Profiles of carbohydrate and protein generation under different nutrient conditions: (a) carbohydrates/TOC in EOM; (b) carbohydrates/TOC in IOM; (c) proteins/TOC in EOM; and (d) proteins/TOC in IOM.

TOC in IOM was much higher than that in EOM in both the stationary and the decline phases, which differs from the pattern observed in the carbohydrate profiles and is probably due to the incomplete release of protein from the algae cells. In EOM, the proportion of protein in TOC in the stationary phase was zero (the protein yield was lower than the limit of detection (0.01913 mg/L), under the concentration of phosphorus as 0.01, 0.20, 1.00 mg/L, respectively. The corresponding values increased to 0.28, 2.02 and 1.63 in the decline phase. The trend in the variation of the protein concentrations in the IOM was similar to that observed for the EOMs, namely lower in the stationary phase and higher in the decline phase. This indicates that the nitrogen concentration is the important factor governing the generation and release of protein. It also suggests that the provision of sufficient phosphorus is more beneficial for *N. palea* growth as it allows the use of the ambient nitrogen in the medium to generate protein in AOM than under solely nitrogen conditions. Moreover, when the ambient nitrogen is sufficient, the protein content of both the EOM and the IOM increases as the phosphorus concentration increases. This indicates that the absorption of nitrates by the algae in the medium may be strongly influenced by the availability of phosphate. This biological reaction also plays an important role in the generation of ATP and in the activities of many enzymes, which are known to significantly influence the generation of carbohydrates and proteins of algae (Huang et al., 2012). Based on this analysis of cell growth and TOC, phosphorus acts as the control factor, but for carbohydrates and protein nitrogen is the major factor boosting AOM yields. Compared with other studies focused on *M. aeruginosa* and other diatom species, the value of proteins/TOC as BSA was much higher than 1.0, indicated that more amount of peptide with larger molecular weight would be generated during the growth of *N. palea* (Henderson et al., 2008). The amount of protein calculated as ng/cell of *N. palea*'s AOM, was much lower than that generated from *M. aeruginosa* (Huang et al., 2012), which is different from the results of TOC, indicating that protein and peptide was not the dominated species of AOM generated from *N. palea*.

2.4. Amino acid profile of *N. palea*'s AOM

A substantial input of amino acids in lakes or reservoirs, coming from direct releasing or polypeptide decomposition, has a major impact on the solution pH, reducing the capacity of water self-purification and hindering the growth of microorganisms in the water (Dotson and Westerhoff, 2012). However, although amino acids are an important component of disinfection by-product precursors (Chang et al., 2013; Shan et al., 2012), they have rarely been studied in AOM. Therefore, this study also examined trends in the generation of amino acids in *N. palea* AOM (Fig. 3a). The variation in the total amino acids in the EOM exhibited an interesting trend. Increased nutrient concentration was good for amino acid generation in the EOM as well as for releasing amino acids from IOM, regardless of the nutrient source. Under nitrogen control experiments, the maximum yield of total amino acids was achieved in the exponential phase, but this was achieved in the stationary phase under phosphorus control condition. The total amino acid yield under different phosphorous loadings was much higher than that under nitrogen control experiments. This result contrasted with the findings reported above for carbohydrates and proteins. The phosphorous concentration generally favored amino acid generation. In the decline phase, even the lowest concentration, TP = 0.01 mg/L, boosted the amino acid concentration, probably because of the two additional processes: (1) the photo-dissolution of organic matter and (2) the leaching of particulate organic matter from cell fragments (Leloup et al., 2013). The total amino acids in IOM were barely detectable under any of the nitrogen concentrations throughout all the algae growth phases. This is a sharp contrast with the findings in Section 2.3 for carbohydrates and proteins (Fig. 3). The difference could be due to that the carbohydrates in the IOM accumulated rapidly and were concurrently reduced to free amino acids in the IOM, exhausting the nitrogen from the adaptation to stationary phase, as previous studies (Granum et al., 2002). However, in the rich or too-rich phosphorus experiments, the total amino acids were only detected in the EOM and the yield of the total amino acids decreased from the exponential phase to the stationary
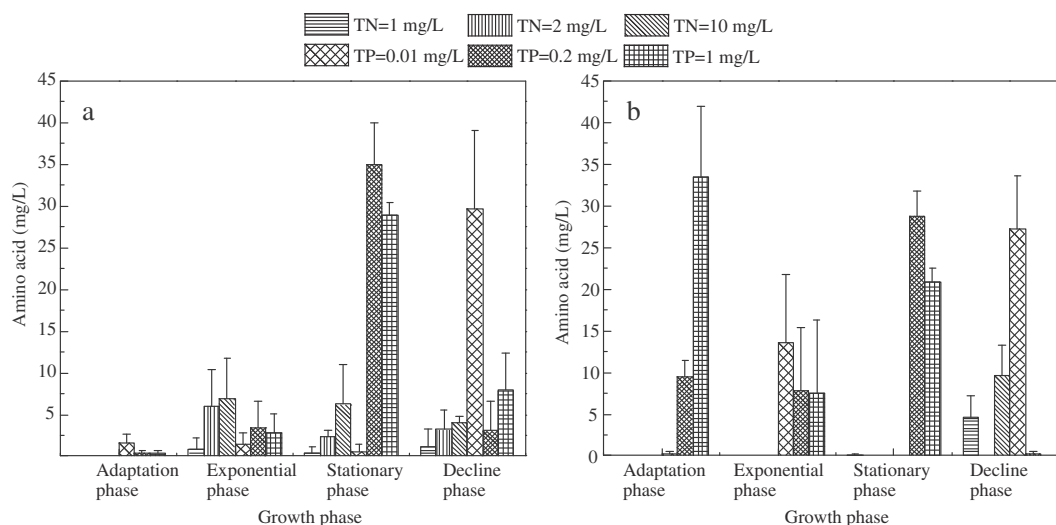

Fig. 3 – Profiles of amino acids generation under different nutrient conditions in: (a) EOM; and (b) IOM.

one, after which it increased significantly in the stationary phase. Amino acids are synthesized by algal cell during the initial growth and are utilized by the algal cell to crack grow, leading to a decrease during the exponential phase. In the stationary phase, the ambient nutrition is insufficient to maintain algae growth, so the amino acids accumulate in the cell as IOM (Droop, 1974). In summary, in both the EOM and IOM, phosphorus supports the generation and release of amino acids.

2.5. Identification of N. palea's AOM by fluorescence spectroscopy

2.5.1. EEM spectra
Fluorescence EEM spectra is an effective method to characterize the organic components in NOMs. Generally, EEM spectra can be divided into 5 regions (Zhang et al., 2013) as Region I (Ex/Em: 200–250 nm/270–330 nm) and II (Ex/Em: 200–250 nm/330–380 nm) corresponded to aromatic proteins, respectively; Region III (Ex/Em: 200–250 nm/380–500 nm) was associated with fulvic acid (FA)-like substances; and Regions IV (Ex/Em: 250–280 nm/270–380 nm) and V (Ex/Em: 250–400 nm/380–500 nm) represented the soluble microbial products (SMPs, e.g., proteins and polysaccharide-like materials) and humic acid (HA)-like substances, respectively. The EOM and IOM extracts of N. palea at the different phases under different nitrogen or phosphorus loadings exhibited distinctly different spectral characterization (Appendix A Fig. S2). Under different phosphorus concentrations, all five regions were detected in the EOM samples, and aromatic proteins and SMPs (Regions I, II and IV) were the main substance found in the IOM. As the phosphorus concentration increased, the fluorescence intensity of the HA-like substances (Region V) in the IOM followed a significant pattern, first increasing and then declining. In the EOM, the variation of the phosphorus concentration significantly changed the fluorescence intensity of all five of the different substances. So did the growth phases. Under different nitrogen concentrations, aromatic proteins, FA-like substances and SMPs (Regions I, II and IV) are the main constituents of EOM and IOM. The nitrogen loading and algal growth phase affect the fluorescence intensity of the above substance in the EOM and IOM. The intensity of the HA-like substance in IOM in the exponential phase increased with increasing nitrogen concentration, but weakened significantly from the exponential phase to stable phase under the TN was 10 mg/L. The effect of ambient phosphorus was clearly greater on the composition of AOM than that of nitrogen. The variation of EEM spectra under different nutrition loadings is likely due to the variation of the chemical composition and/or the molecular weight distribution of AOMs over the algal growth phase (Zhang et al., 2013).

The FRI method was used to quantitatively analyze the EEM fluorescence characteristics of N. palea AOMs (Fig. 4). In all the samples tested, the aromatic proteins (I and II) and SMPs (IV) were the main components in both the EOM and IOM, with SMPs being the most important component of the five substances. This result indicated that the nitrogen contained substance was generated in IOM and released into EOM. The carbon contained substance was not the dominated substance caused fluorescence signal. This result was consistent with AOMs generated from M. aeruginosa and chlorella.

Increasing the nitrogen or phosphorus concentration increased the SMP yield, regardless of the growth phase. The nutrient loading effect was more significant for the EOM. The presence of both dead and new algae cells in the decline phase, seriously affected the generation profiles of the AOM. Therefore, EEM results in decline phase were not compared with other growth phases. The aromatic proteins (I and II) in the EOM achieved their maximum values under the three different phosphorus concentrations in the exponential, stationary and stationary phases, respectively. This indicates that increasing the phosphorus concentration is beneficial for the generation of aromatic proteins in the EOM in the stationary phase. The aromatic proteins (I and II) in the IOM all reached their maximum value in the exponential phase, suggesting that the aromatic proteins were generated more remarkably in this phase. When the ambient nitrogen is sufficient, the aromatic proteins in the IOM are mainly generated in the exponential phase regardless of the ambient phosphorus concentration. As is clearly shown in Fig. 4a and b), the variation in the concentrations of the aromatic proteins in the EOM was more significant than that in the IOM. This may be because N. palea mostly releases the aromatic proteins from the IOM to the EOM. The aromatic proteins in the EOM achieve their maximum value under the 3 different nitrogen concentrations in the stationary, stationary and exponential phases respectively. In contrast, the aromatic proteins (I and II) in the IOM reach their maximum value in the exponential, adaptation and adaptation phases, respectively. This indicates that decreasing the nitrogen concentration is beneficial for the generation of aromatic proteins in the EOM during the stationary phase. However, increasing the nitrogen concentration is beneficial for the generation of aromatic proteins (I and II) in the IOM in the adaptation phase. Under the different nitrogen loadings, the concentrations of the aromatic proteins (I and II) in the EOM varied more significantly than in the IOM. This follows the same pattern as the different phosphorus concentrations, which indicates that the aromatic proteins (I and II) in the EOM are released by the IOM to achieve this growth, regardless of the nitrogen and phosphorus concentrations. As the nitrogen concentration increased, the aromatic proteins (I and II) in the EOM declined sharply. At the highest nitrogen concentration of 10 mg/L, the aromatic proteins (I) were hardly detectable in the adaptation phase and the aromatic proteins (II) were also very low. These results indicate that as long as the ambient phosphorus concentration is sufficient, increasing the nitrogen concentration will be more beneficial for N. palea's consumption of aromatic proteins (I and II) in the EOM than increasing the phosphorus concentration. Under different nitrogen and phosphorus concentrations, the proportion of aromatic proteins (I and II) was reduced as the proportion of SMPs increased. This phenomenon was most significant for the highest TN of 10 mg/L, where the proportion of SMPs reached 85% in the adaptation and decline phases. Overall, as long as the ambient phosphorus concentration is sufficient, changing the nitrogen concentration will have a more significant impact on the EOM composition and is more beneficial for N. palea's ability to generate SMPs in both its EOM and IOM. Under different nitrogen and phosphorus concentrations the proportion of aromatic proteins (I and II) reduced as the
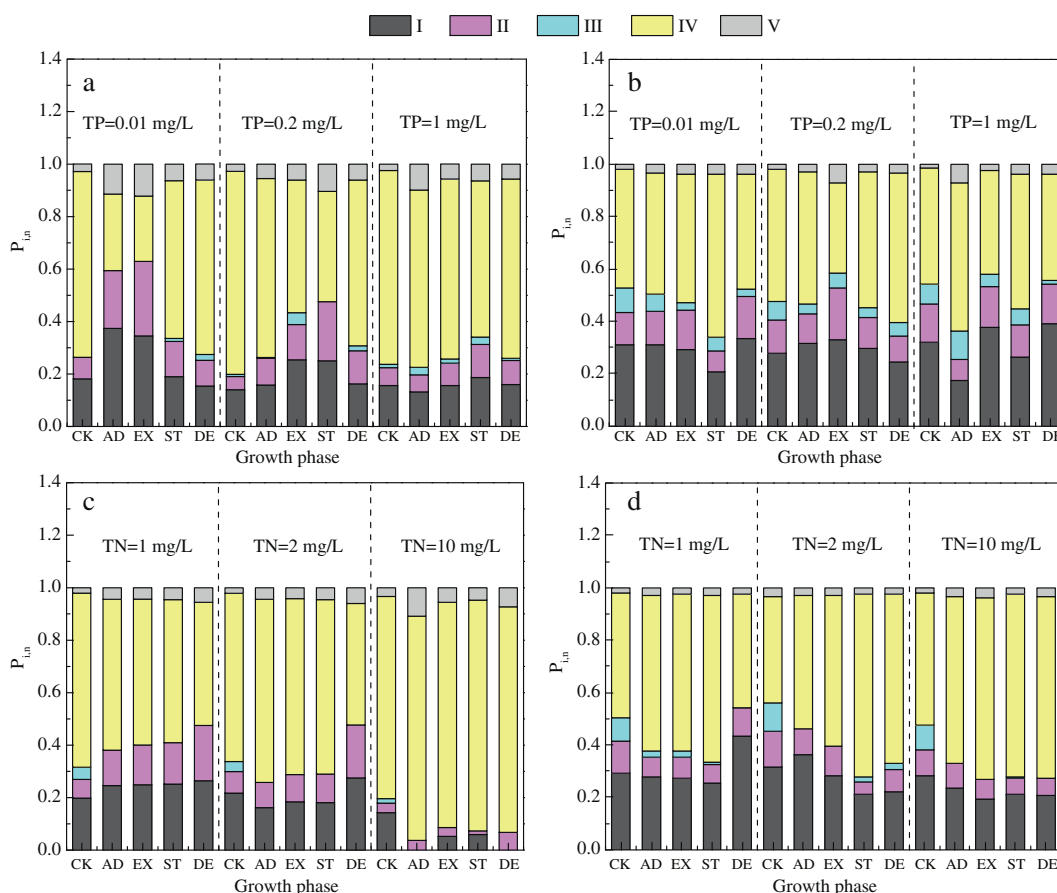
Fig. 4 – The fluorescence response ($P_{i, n}$) for five different regions in the Excitation-emission fluorescence (EEM) spectra under different nutrient conditions: (a) and (c) sampling from EOM, (b) and (d) sampling from IOM; AD: adaptation phase; EX: exponential phase; ST: stationary phase; DE: decline phase.

proportion of SMPs increased. The integrate content of FA-like substances and humic substances were less than 40% under all nutrient loading and growth phase, indicating that humus in AOMs of *N. palea* was not the dominate species as other algae.

2.5.2. Synchronous fluorescence spectra
In general, SF represents the summation of several different fluorescence characteristics shown by organic matter, and they provide better resolution and more highly detailed information than the EEM spectra (He et al., 2011). In Fig. 5, three main regions were identified in *N. palea* AOM, Region A (250–308 nm), named as the protein-like region, is associated with the presence of proteinaceous substance and mono-aromatic compounds (dos Santos et al., 2010); Region B (308–363 nm), was related to the fulvic-like region in that there were the polycyclic aromatics with three to four fused benzene rings and two to three conjugated systems in unsaturated aliphatic structures (dos Santos et al., 2010; Peuravuori et al., 2002); and Region C (363–595 nm) named as humic-like substances, corresponds to polycyclic aromatics with approximately 5–7 fused benzene rings (Peuravuori et al., 2002).

In the protein-like region of the EOM (Fig. 5), there is a red shift in the maximum fluorescence intensity relative to the

adaptation phase that varies significantly under different phosphorus concentrations with the growth of *N. palea*. Organic substances with fluorescence signals at short wavelengths corresponded to the simple structural components with a lower degree of aromatic polycondensation and lower molecular weight (He et al., 2011). On the contrary, fluorescence signals at long wavelengths correspond to complex structural components with a higher degree of conjugation and higher molecular weight. This red shift of fluorescence intensity can be attributed to an increase in aromatic group condensation in these molecules (Kalbitz et al., 1999). AOMs with a higher degree of aromatic polycondensation generally exhibit higher chemical stability, thus increasing the retention time of AOMs in lakes (dos Santos et al., 2010) and consequently influencing the chemical composition of lake water. However, when ambient nitrogen and phosphorus concentrations were 2 and 0.2 mg/L, this red shift for EOM was not very significant indicating that aromatic group condensation of the protein-like substance of the EOM is not favored. Interestingly, although this shift of the protein-like region was not detected in the IOM under different phosphorus concentrations, it was also observed in both the EOM and IOM for different nitrogen concentrations. This suggests that the internal environment of the cell is stable and thus not conducive to changing the structure of the IOM. Hence,
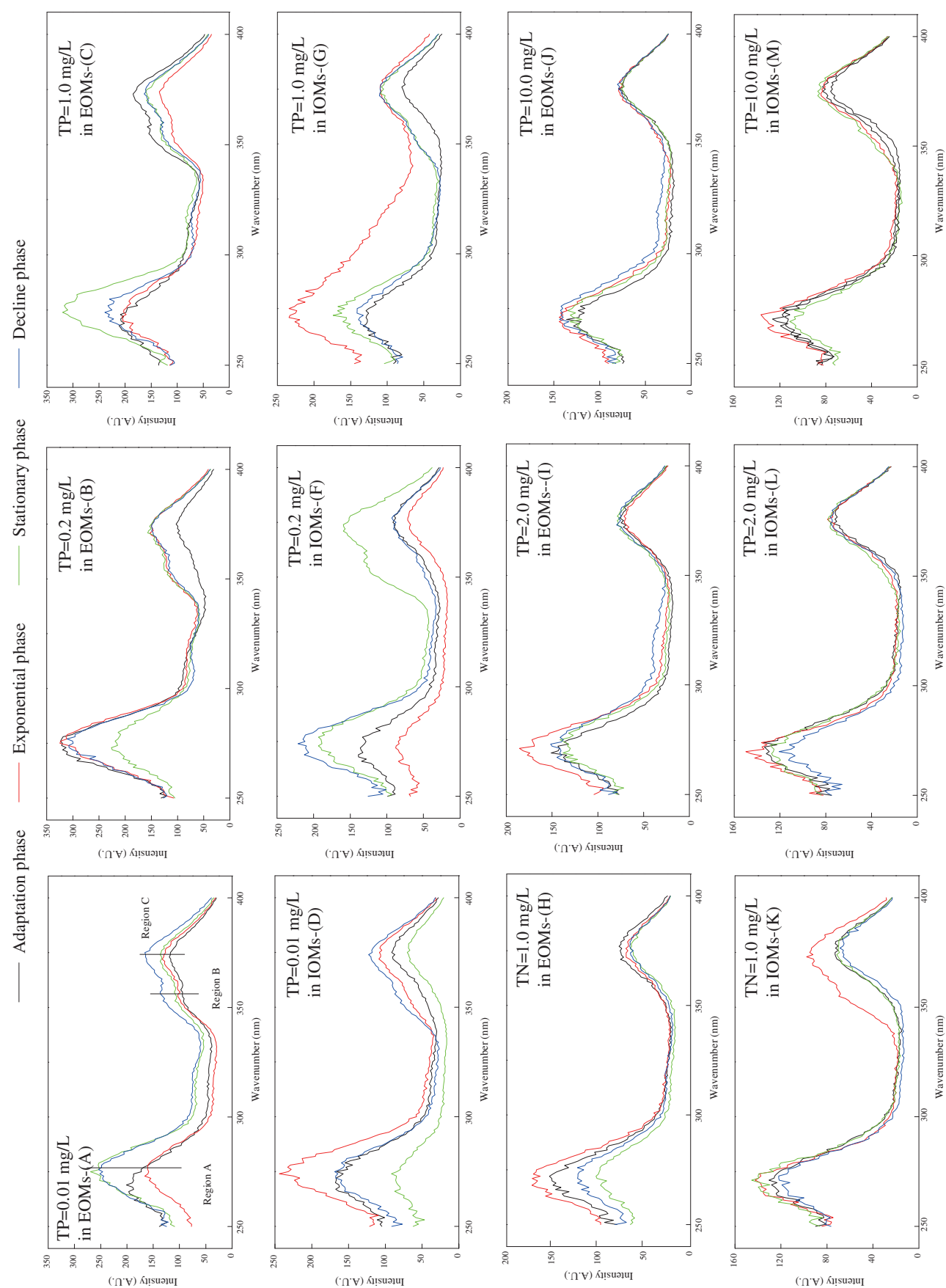
Fig. 5 – Synchronous fluorescence spectra of EOM and IOM under different nutrient conditions.

when the ambient phosphorus concentration is sufficient, no significant variation of the structure of the EOM with the changing of nitrogen loading was observed. In addition, the data revealed that protein-like material (Region A) was the main component of the *N. palea* AOM. Under different phosphorus concentrations, the variations in Region A (protein-like), Region B (fulvic acids) and Region C (humic-like) are clear for both the EOM and IOM, although this was only observed under the poor nitrogen concentration for IOM in the exponential phase. The peak for region B (fulvic acids) was barely detectable in either the EOM or IOM under different nitrogen concentrations. This confirms the result shown in Fig. 4c and d. The FA-like substances were barely detectable in the EOM under different nitrogen concentrations, but decreased in IOM samples as the nitrogen concentration increased, indicating that the ambient nitrogen concentration will have an impact on the generation and accumulation of FA-like substances in the IOM.

2.5.3. UV spectra

Modeling results for the UV spectra of AOMs under different nitrogen and phosphorus concentrations are shown in Fig. 6, including two fitted curves for EOM under conditions of TP = 1.0 mg/L and TN = 10.0 mg/L, respectively. Detailed information of the different nutrient conditions and growth phases is provided in Table 1. However, the intensity of the UV spectra in all the IOM samples was too low to be analyzed by the above mathematical method. A typical result of a failed fitting for an IOM sample (under TP = 1.0 mg/L) is shown in Appendix A Fig. S3. As a result, the UV spectra of the IOM samples will not be discussed by this mathematical method.

As shown in Table 1, the Gaussian bands at 200, 204, 206, 216, 218, 226, 230, 232, 234, 246, 284 and 296 nm all appear in the EOM spectra of *N. palea* under different nitrogen and phosphorus concentrations. As most detectable UV absorbance in organic compounds or functional group is based on the transitions of $n \rightarrow \pi^*$ or $\pi \rightarrow \pi^*$, the energies required for these processes lead to the absorption peaks from 200 to 700 nm (Her et al., 2002). Generally, three specific bands in the UV region for $\pi \rightarrow \pi^*$ transitions were observed in many organic matters: the electron-transfer (ET) band (254 nm), the benzenoid (BZ) band (203 nm) and the local excitation (LE) band (180 nm). Yan et al.

(2012) found that in dissolved organic matter (DOM) the absorption maxima wavelength of 206 nm corresponds to the $n \rightarrow \pi^*$ transition for carboxylic acid and esters in water. Many of the compounds that have been identified in SMPs are aromatic (Kunacheva and Stuckey, 2014), and Carvallo et al. (Carvallo et al., 2007) found that UV–Vis absorbance at wavelengths between 250 and 207 nm can be a useful way to estimate the concentration of SMPs. The absorption band can be enhanced depending upon the substituent type and its position on the unsaturated carbonyl chromophore (Her et al., 2008). We therefore speculated that the Gaussian bands at 200, 204 and 206 nm were corresponded to carboxylic acid and esters, while those at 216, 218 and 226 nm represented a benzene ring substituted with $-OCH_3$, $-SO_2NH_2$ and $-CN$, respectively. The bands at 230 and 232 nm represented a benzene ring substituted with $-NH_2$; that at 234 nm represented a benzene ring substituted with $-O^-$; and the band at 246 nm represented a benzene ring substituted with $-COCH_3$ (Friedel and Orchin, 1951; Hirayama, 1967; Silverstein and Webster, 2006). Generally, ultraviolet absorption characteristic peaks for carbonyl groups occurred in the region 270–300 nm (Hirayama, 1967), and an ultraviolet absorption band of a benzene ring substituted with $-O^-$ was at 287 nm and an ultraviolet absorption band for phenylacetic and 2,5-dihydroxy substitutions were at 290 nm (Hirayama, 1967; Silverstein and Webster, 2006). Hence, the Gaussian band at 284 nm likely represented carbonyl or phenol-like compounds, while that at 296 nm represented one or more of carbonyl, phenylacetic and 2,5-dihydroxy. All the above speculations concerning the functional groups represented by the different Gaussian peaks, are based on substituted benzene rings. In addition, the phenyl ring substitution of aromatic substances and the effect of conjugated fused ring phenomenon effect cannot be ignored and thus requires further discussion.

As shown in Table 1, the functional groups of carboxylic acid and esters, a benzene ring substituted with $-SO_2NH_2$ and a benzene ring substituted with $-NH_2$ are mainly present in different growth phases and under different phosphorus concentrations, except for the adaptation phase of the TP = 0.01 mg/L condition. When the ambient phosphorus supply was poor (TP = 0.01 mg/L), the EOM consisted of carboxylic acid
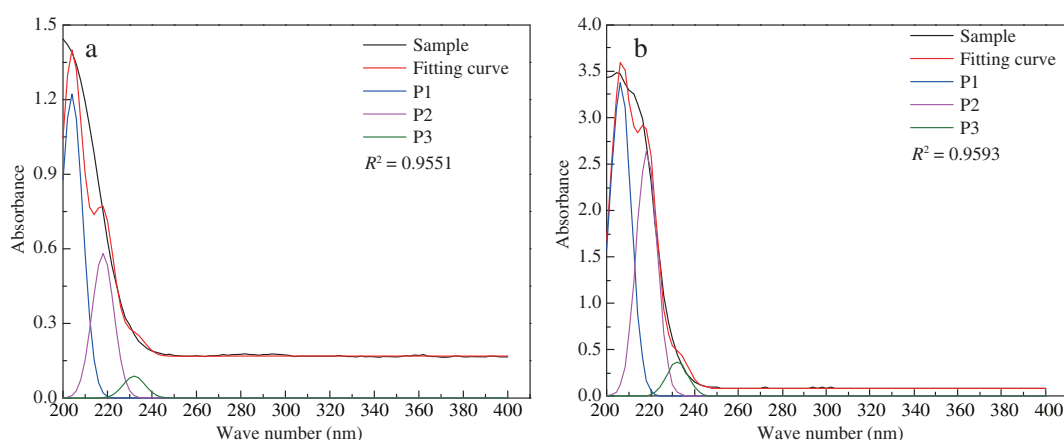

Fig. 6 – Gaussian band fitting of the UV spectra of EOM for two different nitrogen/phosphorus concentrations: (a) TP = 1 mg/L; (b) TN = 10 mg/L.

Table 1 – Gaussian components and fitting of UV spectra for algal organic matters (AOMs) for different nitrogen/phosphorus concentrations and growth phases.

	Adaptation phase		Exponential phase		Stationary phase		Decline phase	
	Position of maximum λ (nm)	Area	Position of maximum λ (nm)	Area	Position of maximum λ (nm)	Area	Position of maximum λ (nm)	Area
TP = 0.01 mg/L	200	1.1452	204	5.5933	204	6.3007	204	6.3359
TN = 2 mg/L	216	6.4826	218	5.5407	218	5.8466	218	5.8339
	230	1.3300	232	1.3090	232	1.1360	232	1.0640
	296	0.1433	246	0.2059				
	$R^2 = 0.8640$		$R^2 = 0.9643$		$R^2 = 0.9558$		$R^2 = 0.9569$	
TP = 0.2 mg/L	204	6.5506	200	1.1186	204	5.7315	204	6.5144
TN = 2 mg/L	218	6.9025	218	5.2387	218	6.7748	218	6.8744
	232	1.0575	232	1.0356	232	1.1284	232	1.2178
			246	0.1246				
			284	0.1333				
	$R^2 = 0.9563$		$R^2 = 0.8472$		$R^2 = 0.9565$		$R^2 = 0.9578$	
TP = 1 mg/L	204	5.3663	204	6.3403	204	6.1376	204	6.0194
TN = 2 mg/L	218	6.7782	218	5.8664	218	5.9317	218	6.7552
	232	1.0052	232	1.1358	232	1.0702	232	1.0877
	$R^2 = 0.9556$		$R^2 = 0.9558$		$R^2 = 0.9553$		$R^2 = 0.9551$	
TN = 1 mg/L	206	5.1492	206	5.2042	206	4.6007	206	4.7067
TP = 1 mg/L	232	0.8331	226	1.5448	234	0.6097	232	0.7599
	$R^2 = 0.9456$		$R^2 = 0.9564$		$R^2 = 0.9449$		$R^2 = 0.9425$	
TN = 2 mg/L	206	0.9348	206	9.3693	206	9.6977	206	9.4094
TP = 1 mg/L	232	1.1154	234	1.0429	232	1.2144	232	1.2690
	$R^2 = 0.9434$		$R^2 = 0.9596$		$R^2 = 0.9435$		$R^2 = 0.9435$	
TN = 10 mg/L	206	23.9469	206	8.2910	206	8.3348	206	8.2308
TP = 1 mg/L	218	31.9621	218	26.9909	218	31.5692	218	31.9221
	232	4.2725	232	4.3246	232	4.1014	232	4.3996
	$R^2 = 0.9581$		$R^2 = 0.9585$		$R^2 = 0.9579$		$R^2 = 0.9593$	

UV: ultraviolet; TP: total phosphorous; TN: total nitrogen.

and esters, a benzene ring substituted with –OCH$_3$, and a benzene ring substituted with –NH$_2$ or carbonyl, phenylacetic or 2,5-dihydroxy in the adaptation phase. In addition, a benzene ring substituted with –COCH$_3$ was present in the exponential phase of the TP = 0.01 mg/L condition and a benzene ring substituted with –COCH$_3$ and carbonyl or phenol salt compounds were present in the exponential phase (TP = 0.2 mg/L). Only two types of molecules, carboxylic acid and esters and a benzene ring substituted with –NH$_2$, were present in different growth phases for TN = 1 mg/L and TN = 2 mg/L, except for the exponential and stationary phases (under TN = 1 mg/L) and the exponential phase (under TN = 2 mg/L). When the ambient nitrogen was too rich (TN = 10 mg/L), there were three types of molecules, such as carboxylic acid and esters, a benzene ring substituted with –SO$_2$NH$_2$ and a benzene ring substituted with –NH$_2$. In addition, a benzene ring substituted with –CN existed in the exponential phase of the TN = 1 mg/L condition and a benzene ring substituted with –O$^-$ was present in both the stationary phase (under TN = 1 mg/L) and the exponential phase (under TN = 2 mg/L). The area of the different Gaussian bands ranged from 0.5 to 7 under different phosphorus concentrations, and the area of different Gaussian bands from 0.5 to 32 under different nitrogen concentrations. In addition, the variation of peak area in the different Gaussian bands was much smaller for changing phosphorus concentrations than that for different nitrogen levels. This indicates that when the ambient phosphorus concentration is sufficient, increasing the nitrogen concentrations is beneficial as it allows *N. palea* to accumulate representative material such as carboxylic acid and

esters, a benzene ring substituted with –SO$_2$NH$_2$ and a benzene ring substituted with –NH$_2$.

3. Conclusions

Based on the detailed investigation of *N. palea*'s AOM presented here, two major conclusions can be reached: (1) as long as the ambient nitrogen is sufficient, increasing the phosphorus concentration is beneficial for *N. palea* growth, which is mainly reflected in the extension of the exponential phase. It is also beneficial for the generation of amino acids and TOC in both its EOM and IOM. As long as the ambient phosphorus concentration is sufficient, increasing the nitrogen is beneficial for *N. palea* growth, as it enables to generate/accumulate protein and carbohydrates in both EOM and IOM. Based on the above observations, phosphorus is the more important nutrient factor affecting *N. palea*'s growth and the composition of its AOMs.

(2) Synchronous fluorescence spectroscopy and deconvolution UV–vis spectrum were used for the characterization of the AOM firstly. The results of the synchronous fluorescence spectroscopy revealed that different phosphorus concentrations changed the structure of the protein-like substance in EOM, leading to an increase in aromatic group condensation in the protein-like substance. The results of the UV–vis spectroscopy revealed the existence of carboxylic acid and esters in EOM and the phenylacetic and 2,5-dihydroxy may also be present from the observation of the long wavelength UV absorbance. There was

also evidence to suggest the presence of the functional groups –OCH_3, –SO_2NH_2, –CN, –NH_2, –O^- and –$COCH_3$ substituted onto the benzene ring in EOM.

Acknowledgments

Appendix A. Supplementary data

Supplementary data to this article can be found online at http://dx.doi.org/10.1016/j.jes.2016.02.002.

REFERENCES

Alizadeh Tabatabai, S.A., Schippers, J.C., Kennedy, M.D., 2014. Effect of coagulation on fouling potential and removal of algal organic matter in ultrafiltration pretreatment to seawater reverse osmosis. Water Res. 59, 283–294.

Beaulieu, S.E., Sengco, M.R., Anderson, D.M., 2005. Using clay to control harmful algal blooms: deposition and resuspension of clay/algal flocs. Harmful Algae 4, 123–138.

Cardozo, K.H.M., Guaratini, T., Barros, M.P., Falcao, V.R., Tonon, A.P., Lopes, N.P., et al., 2007. Metabolites from algae with economical impact. Comp. Biochem. Physiol. C Toxicol. Pharmacol. 146, 60–78.

Carvallo, M.J., Vargas, I., Vega, A., Pizarr, G., Pasten, P., 2007. Evaluation of rapid methods for in-situ characterization of organic contaminant load and biodegradation rates in winery wastewater. Water Sci. Technol. 56, 129–137.

Chang, H., Chen, C., Wang, G., 2013. Characteristics of C-, N-DBP formation from nitrogen-enriched dissolved organic matter in raw water and treated wastewater effluent. Water Res. 47, 2729–2741.

Chen, W., Westerhoff, P., Leenheer, J.A., Booksh, K., 2003. Fluorescence excitation–emission matrix regional integration to quantify spectra for dissolved organic matter. Environ. Sci. Technol. 37, 5701–5710.

Chen, X., Zhou, W., Pickett, S.T.A., Li, W., Han, L., Ren, Y., 2016. Diatoms are better indicators of urban stream conditions: a case study in Beijing, China. Ecol. Indic. 60, 265–274.

Chutipongtanate, S., Watcharatanyatip, K., Homvises, T., Jaturongkakul, K., Thongboonkerd, V., 2012. Systematic comparisons of various spectrophotometric and colorimetric methods to measure concentrations of protein, peptide and amino acid: detectable limits, linear dynamic ranges, interferences, practicality and unit costs. Talanta 98, 123–129.

Dokulil, M.T., Teubner, K., 2000. Cyanobacterial dominance in lakes. Hydrobiologia 438, 1–12.

dos Santos, L.M., Simoes, M.L., de Melo, W.J., Martin-Neto, L., Pereira-Filho, E.R., 2010. Application of chemometric methods in the evaluation of chemical and spectroscopic data on organic matter from oxisols in sewage sludge applications. Geoderma 155, 121–127.

Dotson, A., Westerhoff, P., 2012. Character and treatment of organic colloids in challenging and impacted drinking water sources. J. Environ. Eng. 138, 393–401.

Droop, M., 1974. The nutrient status of algal cells in continuous culture. J. Mar. Biol. Assoc. U. K. 54, 825–855.

Fang, J., Ma, J., Yang, X., Shang, C., 2010. Formation of carbonaceous and nitrogenous disinfection by-products from the chlorination of *Microcystis aeruginosa*. Water Res. 44, 1934–1940.

Friedel, R.A., Orchin, M., 1951. Ultraviolet Spectra of Aromatic Compounds. John Wiley.

Glibert, P.M., Icarus Allen, J., Artioli, Y., Beusen, A., Bouwman, L., Harle, J., et al., 2014. Vulnerability of coastal ecosystems to changes in harmful algal bloom distribution in response to climate change: projections based on model analysis. Glob. Chang. Biol. 20, 3845–3858.

González López, C.V., García, M.d.C.C., Fernández, F.G.A., Bustos, C.S., Chisti, Y., Sevilla, J.M.F., 2010. Protein measurements of microalgal and cyanobacterial biomass. Bioresour. Technol. 101, 7587–7591.

Granum, E., Kirkvold, S., Myklestad, S.M., 2002. Cellular and extracellular production of carbohydrates and amino acids by the marine diatom *Skeletonema costatum*: diel variations and effects of N depletion. Mar. Ecol. Prog. Ser. 242, 83–94.

Guerrini, F., Cangini, M., Boni, L., Trost, P., Pistocchi, R., 2000. Metabolic responses of the diatom *Achnanthes brevipes* (Bacillariophyceae) to nutrient limitation. J. Phycol. 36, 882–890.

Guerrini, F., Mazzotti, A., Boni, L., Pistocchi, R., 1998. Bacterial-algal interactions in polysaccharide production. Aquat. Microb. Ecol. 15, 247–253.

He, X., Xi, B., Wei, Z., Guo, X., Li, M., An, D., et al., 2011. Spectroscopic characterization of water extractable organic matter during composting of municipal solid waste. Chemosphere 82, 541–548.

Henderson, R.K., Baker, A., Parsons, S.A., Jefferson, B., 2008. Characterisation of algogenic organic matter extracted from cyanobacteria, green algae and diatoms. Water Res. 42, 3435–3445.

Henderson, R.K., Parsons, S.A., Jefferson, B., 2010. The impact of differing cell and algogenic organic matter (AOM) characteristics on the coagulation and flotation of algae. Water Res. 44, 3617–3624.

Her, N., Amy, G., Foss, D., Cho, J., 2002. Variations of molecular weight estimation by HP-size exclusion chromatography with UVA versus online DOC detection. Environ. Sci. Technol. 36, 3393–3399.

Her, N., Amy, G., Sohn, J., von Gunten, U., 2008. UV absorbance ratio index with size exclusion chromatography (URI-SEC) as an NOM property indicator (vol 57, pg 35, 2008). J. Water Supply Res. Technol. AQUA 57, 289-289.

Hirayama, K., 1967. Handbook of Ultraviolet and Visible Absorption Spectra of Organic Compounds. Plenum Press Data Division, New York.

Huang, W., Chu, H., Dong, B., 2012. Characteristics of algogenic organic matter generated under different nutrient conditions and subsequent impact on microfiltration membrane fouling. Desalination 293, 104–111.

Ishikawa, A., Furuya, K., 2004. The role of diatom resting stages in the onset of the spring bloom in the East China Sea. Mar. Biol. 145, 633–639.

Kalbitz, K., Geyer, W., Geyer, S., 1999. Spectroscopic properties of dissolved humic substances — a reflection of land use history in a fen area. Biogeochemistry 47, 219–238.

Kunacheva, C., Stuckey, D.C., 2014. Analytical methods for soluble microbial products (SMP) and extracellular polymers (ECP) in wastewater treatment systems: a review. Water Res. 61, 1–18.

Labanowski, J., Feuillade, G., 2011. Dissolved organic matter: precautions for the study of hydrophilic substances using XAD resins. Water Res. 45, 315–327.

Laurentin, A., Edwards, C.A., 2003. A microtiter modification of the anthrone-sulfuric acid colorimetric assay for glucose-based carbohydrates. Anal. Biochem. 315, 143–145.

Leloup, M., Nicolau, R., Pallier, V., Yéprémian, C., Feuillade-Cathalifaud, G., 2013. Organic matter produced by algae and cyanobacteria: quantitative and qualitative characterization. J. Environ. Sci. 25, 1089–1097.

Li, L., Gao, N., Deng, Y., Yao, J., Zhang, K., 2012. Characterization of intracellular & extracellular algae organic matters (AOM) of *Microcystic aeruginosa* and formation of AOM-associated disinfection byproducts and odor & taste compounds. Water Res. 46, 1233–1240.

Liu, T., Chen, Z.L., Yu, W.Z., You, S.J., 2011a. Characterization of organic membrane foulants in a submerged membrane bioreactor with pre-ozonation using three-dimensional excitation–emission matrix fluorescence spectroscopy. Water Res. 45, 2111–2121.

Liu, X., Lu, X.H., Chen, Y.W., 2011b. The effects of temperature and nutrient ratios on *Microcystis* blooms in Lake Taihu, China: an 11-year investigation. Harmful Algae 10, 337–343.

Myklestad, S., Haug, A., 1972. Production of carbohydrates by the marine diatom *Chaetoceros affinis* var. *willei* (Gran) Hustedt. I. Effect of the concentration of nutrients in the culture medium. J. Exp. Mar. Biol. Ecol. 9, 125–136.

Peuravuori, J., Koivikko, R., Pihlaja, K., 2002. Characterization, differentiation and classification of aquatic humic matter separated with different sorbents: synchronous scanning fluorescence spectroscopy. Water Res. 36, 4552–4562.

Pivokonsky, M., Kloucek, O., Pivokonska, L., 2006. Evaluation of the production, composition and aluminum and iron complexation of algogenic organic matter. Water Res. 40, 3045–3052.

Servaites, J.C., Faeth, J.L., Sidhu, S.S., 2012. A dye binding method for measurement of total protein in microalgae. Anal. Biochem. 421, 75–80.

Shan, J., Hu, J., Sule Kaplan-Bekaroglu, S., Song, H., Karanfil, T., 2012. The effects of pH, bromide and nitrite on halonitromethane and trihalomethane formation from amino acids and amino sugars. Chemosphere 86, 323–328.

Silverstein, R., Webster, F., 2006. Spectrometric Identification of Organic Compounds. John Wiley & Sons.

Taylor Eighmy, T., Robin Collins, M., Spanos, S.K., Fenstermacher, J., 1992. Microbial populations, activities and carbon metabolism in slow sand filters. Water Res. 26, 1319–1328.

Vandamme, D., Foubert, I., Fraeye, I., Muylaert, K., 2012. Influence of organic matter generated by *Chlorella vulgaris* on five different modes of flocculation. Bioresour. Technol. 124, 508–511.

Yan, M., Korshin, G.V., 2014. Comparative examination of effects of binding of different metals on chromophores of dissolved organic matter. Environ. Sci. Technol. 48, 3177–3185.

Yan, M., Dryer, D., Korshin, G.V., Benedetti, M.F., 2013. In situ study of binding of copper by fulvic acid: comparison of differential absorbance data and model predictions. Water Res. 47, 588–596.

Yan, M., Korshin, G., Wang, D., Cai, Z., 2012. Characterization of dissolved organic matter using high-performance liquid chromatography (HPLC)-size exclusion chromatography (SEC) with a multiple wavelength absorbance detector. Chemosphere 87, 879–885.

Yang, Q., Xie, P., Shen, H., Xu, J., Wang, P., Zhang, B., 2012. A novel flushing strategy for diatom bloom prevention in the lower-middle Hanjiang River. Water Res. 46, 2525–2534.

Zhang, X., Fan, L., Roddick, F.A., 2013. Influence of the characteristics of soluble algal organic matter released from *Microcystis aeruginosa* on the fouling of a ceramic microfiltration membrane. J. Membr. Sci. 425, 23–29.

Zhang, Y., Yan, R., Zhang, Z., Huang, G., Zhu, D., 2007. Effects of different factors on growth of *Nitzschia palea*. Food Sci. 28, 369–373.

Zhou, S., Shao, Y., Gao, N., Deng, Y., Li, L., Deng, J., Tan, C., 2014. Characterization of algal organic matters of *Microcystis aeruginosa*: biodegradability, DBP formation and membrane fouling potential. Water Res. 52, 199–207.

Zhu, M., Gao, N., Chu, W., Zhou, S., Zhang, Z., Xu, Y., Dai, Q., 2015. Impact of pre-ozonation on disinfection by-product formation and speciation from chlor(am)ination of algal organic matter of *Microcystis aeruginosa*. Ecotoxicol. Environ. Saf. 120, 256–262.